Modelling creep rupture strength of ferritic steel welds

D. Cole, C. Martin-Moran, A. G. Sheard, H. K. D. H. Bhadeshia, and D. J. C. MacKay

Recent changes in the design of steam turbine power plant have necessitated the replacement of bolted flanges with welded joints. The design process therefore requires a knowledge of the creep rupture strength of the weld metal consumed in the welding process. This paper presents a method which can be used to estimate the creep rupture strength of ferritic steel weld metals, from a knowledge of the creep strength of wrought plates. The method is validated using published data.

Mr Cole and Professor Bhadeshia are in the Department of Materials Science and Metallurgy, University of Cambridge, Pembroke Street, Cambridge CB2 3QZ, UK, Mr Martin-Moran is with Allen Steam Turbines, Queens Engineering Works, Ford End Road, Bedford MK40 4JB, UK, Dr Sheard is with Rolls-Royce Industrial and Marine Gas Turbines Ltd, Ansty, Coventry CV7 9JR, UK, and Dr MacKay is at the Cavendish Laboratory, University of Cambridge, Madingley Road, Cambridge CB3 0HE, UK. *Manuscript received 3 May 1999; accepted 17 June 1999.*

INTRODUCTION

The creep rupture life is frequently a fundamental limit on the design of steam turbines for power plant. During steady operation, the steam turbine casing achieves the live steam temperature; the steam pressure is contained within a casing; this gives rise to a steady state stress which at elevated temperatures can cause the casing to fail by a creep mechanism.

The present paper is concerned with small steam turbines (<40 MW), of the kind described by Sheard and Raine.[1] This uses a single casing made in two halves which fit around the turbine rotor; the two halves are connected at a horizontal joint using bolts. This bolting limits the pressure differential (i.e. the difference in pressure across the wall of the casing) which can be tolerated to ~ 70 bar. It is possible to overcome this limitation by using multiple casings, but there is then a dramatic increase in the manufacturing cost.

The conditions currently desired of small steam turbines, 90 bar at 540°C (Ref. 2), are beyond the capability of even the most aggressive horizontal joint bolt design, making it necessary to use an expensive double casing. Fortunately, an alternative to this design was implemented recently by Mason and Sheard[3] for a 30·4 MW steam turbine. The details of this single casing design (Fig. 1), which permits the higher pressure differential, are beyond the scope of the present paper, but there are two points that need to be emphasised in the context of the present work:

(i) as for the usual design, the steam is fed into the appropriate part of the casing via a steam pipe; this pipe is conventionally joined to the casing with a vertical flange joint which is bolted together; the flange has had to be upgraded to tolerate the higher steam pressures involved

(ii) the large flange of the steam pipe and its associated bolting comprise a bulky system, making it difficult to assemble the turbine unit.

To overcome these difficulties, it has been decided to replace the bolted vertical joint by a welded joint. For proprietary reasons, the heat affected zone of the weld is expected to behave identically in creep to the region of steel far from the weld. Therefore, the creep properties of the weld metal itself become the issue. Hence, the aim of the present investigation is to estimate the creep rupture life of the weld metal used in fabricating the joint.

The methodology involves the creation of neural network models which adequately capture the complexity of the creep rupture phenomenon. Such models rely for their training on experimental data, available in large quantities for wrought power plant steels but not for actual weld metals. For this reason, the present paper begins by justifying the use of wrought steel data to estimate weld metal properties. The model is validated later in the paper.

COMPARISON OF WELD METAL AND WROUGHT PLATE

Weld metals and steels of matching composition seem to have similar creep rupture properties. The chemical compositions of weld metals and corresponding steel plates are not very different (Fig. 2). Of course, weld metal will, in general, have higher oxygen and nitrogen concentrations, but the former should not affect creep resistance. Although differences in the nitrogen concentration are important, they can easily be taken into account both in the prediction of carbonitride formation and in the neural network model where nitrogen is an input.

The microstructure of an as deposited weld metal is naturally radically different from that of a wrought steel. However, even this is unimportant, because the severe tempering heat treatments used after the welding procedure essentially wipe out the original microstructure and replace it with one which is tempered and similar to that of the steel plate. It is probably for this reason that the welding process itself is found not to influence the creep rupture life.[5]

CREEP RUPTURE STRENGTH: VARIABLES

The basic principles of alloy design for creep resistance are well established and well founded on experience. The steels must have a stable microstructure which contains fine alloy carbides to resist the motion of dislocations; however, changes are inevitable over the long service time, so there must be sufficient solid solution strengthening to ensure long term creep resistance. There may be other requirements such as weldability and corrosion and oxidation resistance. It is nevertheless difficult to express the design process quantitatively, given the large number of interacting variables.

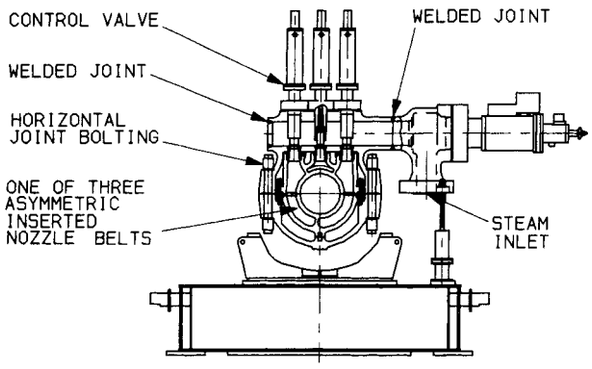

1 Cross-section of advanced high pressure inlet of Mason and Sheard design of steam turbine

The variables taken into account in the present work are listed in Table 1. Note that all information concerned with the prediction of microstructure and properties is, in principle, to be found in this set of parameters, as chemical composition and heat treatments are comprehensively included. There may, of course, be many other independent variables that might be considered important in creep analysis, but these are for the moment neglected for two reasons. First, an empirical analysis requires experimental data; an overambitious list would simply reduce the data set, as publications frequently do not report all of the necessary parameters. Second, the effect of any missing variables would simply be reflected in the uncertainties of prediction. If the predictions are 'noisy' then they can be improved with carefully designed experiments at a future date. Bearing this in mind, the results to be presented are based on some 5420 sets of experiments obtained from the published literature.[6–45] Earlier work on the creep rupture stress of wrought steels by Brun *et al.*[46] used a total of 2066 lines. The present methodology is described briefly below.

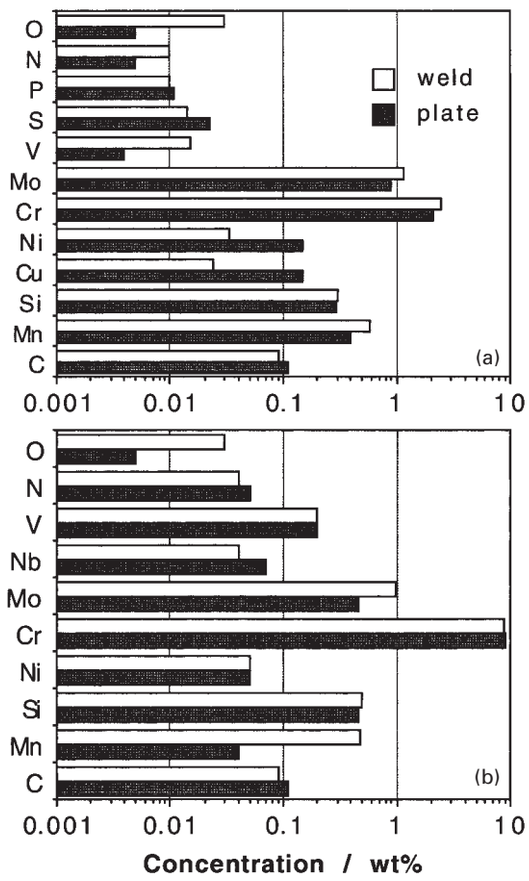

a 2·25Cr–1Mo; *b* 9Cr–1Mo

2 Comparison of chemical compositions of wrought plates and corresponding weld metals of kind used in power plant industry[4]

METHOD

A neural network is a general method of regression analysis in which a very flexible nonlinear function is fitted to experimental data, the details of which have been extensively reviewed.[47] It is nevertheless useful to present some salient features, to place the technique in context.

The flexibility of the non-linear function is related to the number of hidden nodes *i*. Thus, the dependent variable y is given in the present work by

$$y = \sum_{i} w_i^{(2)} h_i + \theta^{(2)} \quad \ldots\ldots\ldots\ldots \quad (1)$$

where

$$h_i = \tanh\left(\sum_{j} w_{ij}^{(1)} x_j + \theta_i^{(1)} \right) \quad \ldots\ldots\ldots \quad (2)$$

where x_j are the j variables on which the output y depends, w_i are the weights (coefficients), and θ_i are the biases (equivalent to the constants in linear regression analysis). The combination of equation (2) with a set of weights, biases, value of i, and the minimum and maximum values of the input variables defines the network completely. Note that the complexity of the function is related to the number of hidden units. The availability of a sufficiently complex and flexible function means that the analysis is not as restricted as in linear regression where the form of the equation has to be defined explicitly before the analysis.

The neural network can capture interactions between the inputs because the hidden units are non-linear. The nature of these interactions is implicit in the values of the weights, but the weights may not always be easy to interpret. For example, there may exist more than just pairwise interactions, in which case the problem becomes difficult to visualise from an examination of the weights. A better method is actually to use the network to make predictions and to see how these depend on various combinations of inputs.

Error estimates

The input parameters are generally assumed in the analysis to be precise, and it is normal to calculate an overall error by comparing the predicted values y_j of the output against those measured t_j, for example

$$E_D \propto \sum_{j} (t_j - y_j)^2 \quad \ldots\ldots\ldots\ldots \quad (3)$$

The error E_D is expected to increase if important input variables have been excluded from the analysis. Whereas E_D gives an overall perceived level of noise in the output parameter, it is, on its own, an unsatisfying description of the uncertainties of prediction.

MacKay has developed a particularly useful treatment of neural networks in a Bayesian framework,[47] which allows the calculation of error bars representing the uncertainty in the fitting parameters. The method recognises that there are many functions that can be fitted or extrapolated into uncertain regions of the input space, without unduly compromising the fit in adjacent regions which are rich in accurate data. Instead of calculating a unique set of weights, a probability distribution of sets of weights is used to define

the fitting uncertainty. The error bars therefore become large when data are sparse or locally noisy.

The error bars presented throughout the present work therefore represent a combination of the perceived level of noise in the output (the creep rupture strength) and the fitting uncertainty as described above.

Overfitting

A potential difficulty with the use of powerful non-linear regression methods is the possibility of overfitting data. To avoid this, the experimental data can be divided into two sets: a training data set and a test data set. The model is produced using only the training data. The test data are then used to check that the model functions when presented with previously unseen data. The training error tends to decrease continuously as the model complexity increases. It is the minimum in the test error that enables the model which generalises best on unseen data to be chosen.[47]

The above discussion of overfitting is rather brief because the problem does not simply involve the minimisation of test error. There are other parameters that control the complexity, which are adjusted automatically to try to achieve the appropriate complexity of model.[47]

ANALYSIS

The aim of the neural network in the present case was to predict the creep rupture stress as a function of the variables given in Table 1. These variables include a comprehensive description of chemical composition and three heat treatments (each characterised by a temperature, duration, and cooling rate from the treatment temperature). If the steel had undergone only two heat treatments, the annealing temperature was set to 300 K to correspond to room temperature. The time to rupture was expressed in logarithmic form, along with the output creep rupture stress, to improve the accuracy of the model.

All 37 different input variables and the output were normalised within the range $\pm 0{\cdot}5$ according to

$$x_{\mathrm{N}} = \frac{x - x_{\min}}{x_{\max} - x_{\min}} - 0{\cdot}5$$

where x is the original value from the database, $x_{\max}$ and $x_{\min}$ are the respective maximum and minimum of each variable in the original data, and x_{N} is the normalised value. This step is not essential to the running of the neural network but later allows a convenient way to compare the results of the output. Figure 3 shows the general structure of the neural network.

Table 1 Details of inputs in database: composition and heat treatments

Variable	Range	Mean	Standard deviation
Test conditions			
log(life, h)	−0·22 – +5·29	3·00	0·28
Temperature, K	723 – 977	867	60·97
Composition			
C, wt-%	0·004 – 0·23	0·11	0·044
S, wt-%	0·01 – 0·86	0·28	0·17
Mn, wt-%	0·01 – 0·92	0·50	0·12
P, wt-%	0·001 – 0·029	0·013	0·0074
S, wt-%	0·001 – 0·02	0·0074	0·0048
Cr, wt-%	2·17 – 12·9	8·20	3·46
Mo, wt-%	0·04 – 2·99	0·84	0·53
Ni, wt-%	0·01 – 2·00	0·23	0·28
Al, wt-%	0·001 – 0·057	0·011	0·012
B, wt-%	0·00 – 0·051	0·0013	0·0041
Co, wt-%	0·00 – 3·09	0·13	0·49
Cu, wt-%	0·01 – 0·87	0·069	0·099
N, wt-%	0·001 – 0·165	0·030	0·027
Nb, wt-%	0·005 – 0·312	0·037	0·045
V, wt-%	0·01 – 0·28	0·13	0·10
W, wt-%	0·01 – 3·93	0·50	0·79
O, wt-%	0·003 – 0·035	0·0099	0·0031
Re, wt-%	0·00 – 1·69	0·014	0·12
Ta, wt-%	0·00 – 0·1	0·0007	0·0066
Normalising			
Temperature, K	1123 – 1453	1283	69·16
Duration, h	0·17 – 33	2·05	3·75
Cooling rate			
in furnace	0 – 1	0·060	0·24
in air	0 – 1	0·58	0·49
oil quenched	0 – 1	0·25	0·43
water quenched	0 – 1	0·11	0·31
Tempering			
Temperature, K	823 – 1133	979	74·88
Duration, h	0·50 – 32	3·64	6·17
Cooling rate			
in furnace	0 – 1	0·060	0·24
in air	0 – 1	0·88	0·33
oil quenched	0 – 1	0·030	0·17
water quenched	0 – 1	0·032	0·18
Annealing			
Temperature, K	300 – 1023	465·7	282·5
Duration, h	0·50 – 50	4·38	8·37
Cooling rate			
in furnace	0 – 1	0·054	0·226
in air	0 – 1	0·946	0·226

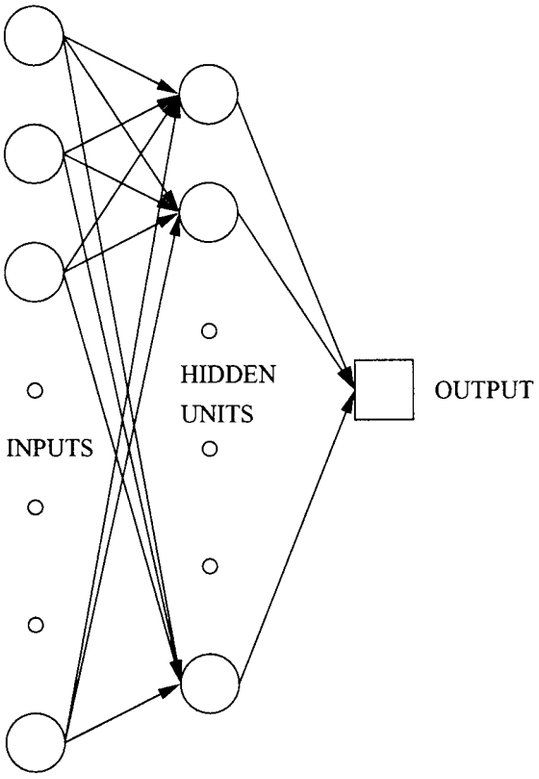

3 Structure of neural network

For several runs of the neural network, Fig. 4*a* shows the model perceived noise σ_v in the creep rupture stress. As expected, σ_v decreases as the fitting function becomes more flexible with larger numbers of hidden units. By contrast, Fig. 4*b* shows that the test error at first decreases and then levels out, with minima at 18–22 hidden units.

Figure 5 shows comparisons made for the best model, consisting of 22 hidden units, using the split database. The comparison of seen data with the model shows very good agreement as should be expected (Fig. 5*a*). The analysis of unseen data by the neural network also shows good agreement (Fig. 5*b*).

The parameter σ_w indicates the importance of an input in terms of its variation having an effect on the output of the model. Figure 6 compares values of σ_w for a selection of inputs for the top five models. A high value of σ_w for a specific input can be caused by the corresponding variable inducing a large variation in the output, but it can be seen from Fig. 6 that different models can assign varying significance to the same input. In such cases, it is possible that a committee of models can make a more reliable prediction than an individual model. The best models are ranked using the values of the test errors. Committees are then formed by combining the predictions of the best L models, where $L=1, 2, \ldots$; the size of the committee is therefore given by the value of L. A plot of the test error of the committee versus its size gives a minimum which defines the optimum size of the committee, as shown in Fig. 7. The test error associated with the best single model is clearly greater than that of any of the committees. It was determined in the present case that a committee of 11 models would be the best choice, being the committee of the lowest test error. The committee was then retrained on the entire data set without changing the complexity of any of its members.

The predictions of the committee trained on the entire data set can be compared with the original data set, as shown in Fig. 8. It can be seen that there is excellent

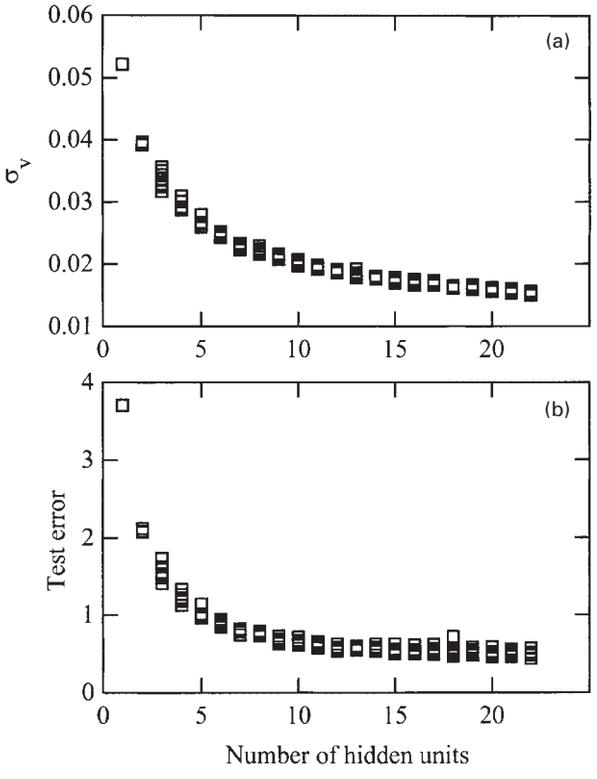

a model perceived noise; *b* test error

4 Model perceived noise and test error as functions of number of hidden units: several values are presented for each set of hidden units because training for each network started with variety of random seeds

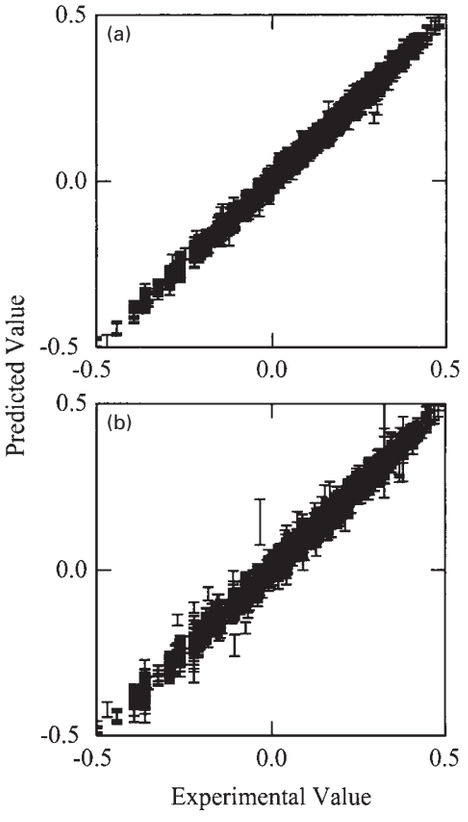

a seen data; *b* unseen data

5 Comparisons of seen and unseen data with model

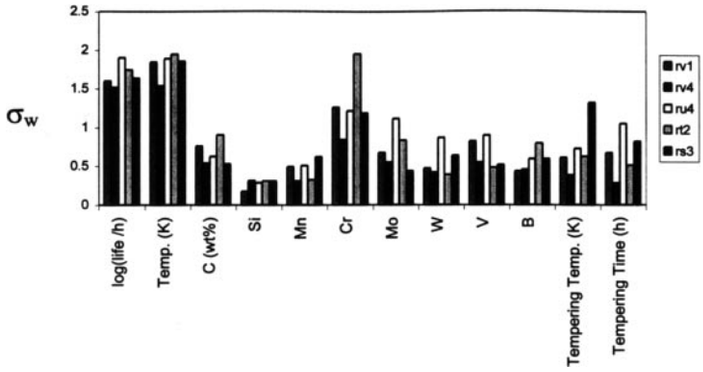

6 Comparison of values of σ_w for top five models

agreement between the values and that the error bars are extremely small.

APPLICATION OF MODEL

Figure 9 shows predictions using the neural network in examining the creep rupture strength of a standard 2·25Cr–Mo steel and a modern 10Cr–Mo–W heat resistant steel (Table 2).

The error bounds in Fig. 9 represent the uncertainty in fitting the non-linear function to the training data, as 65% confidence limits with the σ_v added quadratically. The calculated lifetime of each steel was examined at temperatures of 550, 600, and 650°C. The network correctly predicts

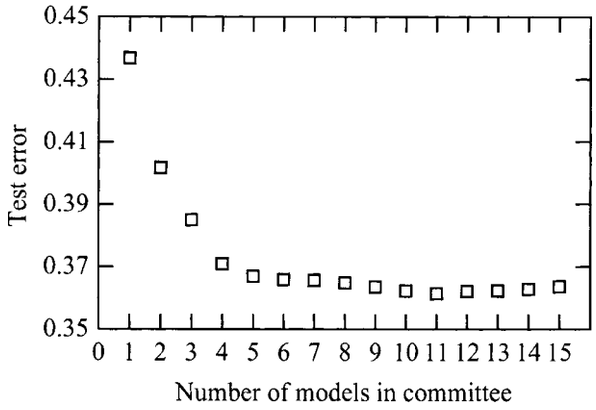

7 Comparison of test errors of increasing size of committee

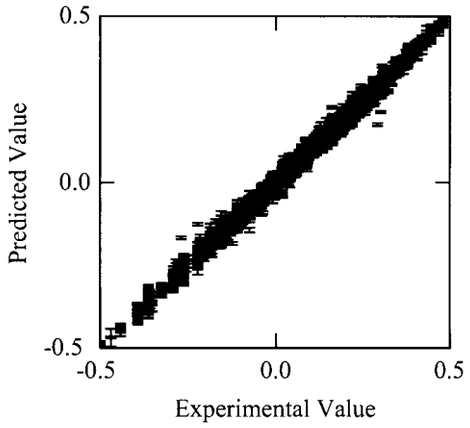

8 Comparison of predicted and experimental values for committee

that the creep strength of the two steels will reduce with increasing lifetime and temperature, and also that the 10Cr–Mo–W steel is more creep resistant than 2·25Cr–Mo. The error bars, represented by dashed lines, are smaller when the neural network is confident of the predictions that it is making. Increases in error bar size, such as at long life for the 2·25Cr–Mo alloy at 650°C (Fig. 9*e*), indicate that a lack of experimental data is restricting the accuracy of the predictions.

The behaviour of the model can be assessed further by examining creep rupture strength of a variety of steels and determining whether the predictions made by the neural network agree with practical results or microstructural theory. In one case, the creep rupture stress of an uncommon 3%Cr steel was examined using the neural network and then compared with the results for the

Table 2 Heat treatments and compositions of two common power plant steels

	2·25%Cr	10%Cr
Normalising		
Temperature, K	1203	1338
Duration, h	6	2
Cooling rate	water quenched	in air
Tempering		
Temperature, K	908	1043
Duration, h	6	4
Cooling rate	in air	in air
Annealing		
Temperature, K	873	1013
Duration, h	2	4
Cooling rate	in air	in air
Composition		
C, wt-%	0·15	0·12
Si, wt-%	0·21	0·05
Mn, wt-%	0·53	0·64
P, wt-%	0·012	0·016
S, wt-%	0·012	0·001
Cr, wt-%	2·4	10·61
Mo, wt-%	1·01	0·44
Ni, wt-%	0·14	0·32
Al, wt-%	0·018	0·022
B, wt-%	0·0003	0·0022
Co, wt-%	0·05	0·015
Cu, wt-%	0·16	0·86
N, wt-%	0·0108	0·064
Nb, wt-%	0·005	0·01
V, wt-%	0·01	0·21
W, wt-%	0·01	1·87
O, wt-%	0·01	0·01
Re, wt-%	0·0003	0·0003
Ta, wt-%	0·0003	0·0003

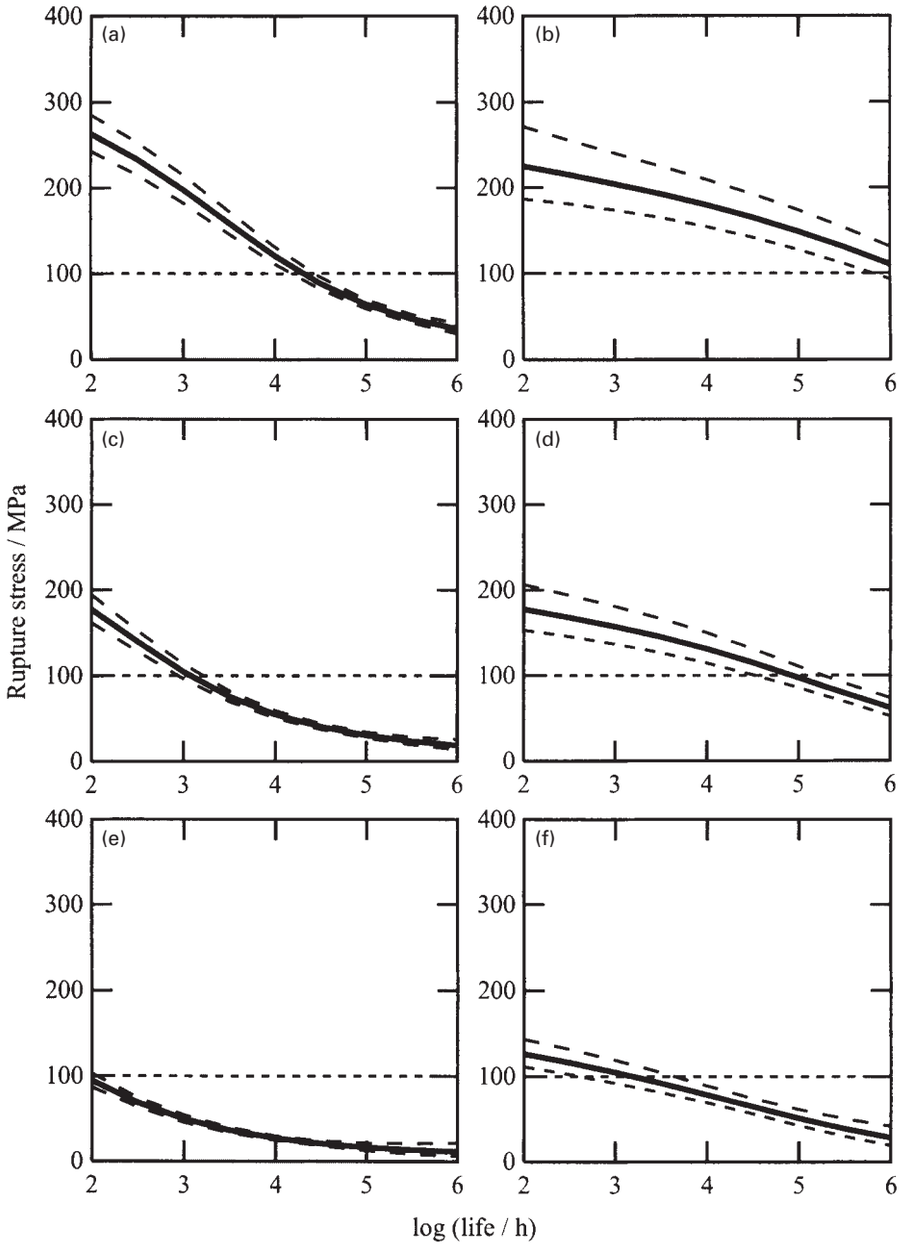

a 2·25Cr–Mo, 550°C; *b* 10Cr–Mo, 550°C; *c* 2·25Cr–Mo, 600°C; *d* 10Cr–Mo, 600°C; *e* 2·25Cr–Mo, 650°C; *f* 10Cr–Mo, 650°C

9 Neural network results for well known power plant steels

2·25%Cr steel examined above. It could be expected that the 3%Cr steel should have a consistently higher creep rupture stress than the 2·25%Cr steel owing to the increase in chromium content, but it can be seen from Fig. 10 that they have comparable creep rupture lives. Figure 10 also shows that the uncertainty for the 3%Cr steel is much greater than that for the 2·25%Cr steel, this being because the amount of information in the database on 3%Cr steel is much less than that on 2·25%Cr steel.

The above phenomenon can be explained by microstructural theory and is an excellent result for the neural network. The microstructural trends were examined by Robson and Bhadeshia;[48] the results of this research are represented in Fig. 11, showing plots of carbide volume fraction versus time for 3%Cr steel and for 2·25%Cr steel. It is apparent that the rate at which $M_{23}C_6$ precipitates in 3%Cr steel is very much greater than that in 2·25%Cr steel. It can also be seen that the maximum volume fraction of M_2X attained by the 3%Cr alloy is much less. These plots show that, in the 2·25%Cr steel, M_2X starts to precipitate well before $M_{23}C_6$, forming a large volume fraction which then suppresses $M_{23}C_6$ formation (Fig. 11*a*). However, in the higher chromium steel both carbides tend to precipitate at similar times, and both phases are then competing for solute (Fig. 11*b*). The $M_{23}C_6$ phase dominates and M_2X dissolves. The M_2X precipitate is considered to be a factor in improving creep rupture strength, whereas $M_{23}C_6$ is considered less effective in resisting creep deformation owing to its large size. This then explains why the 3%Cr steel is not as creep resistant as expected.

The neural network model may be used to examine the influence of any of the input variables on the output. Hence, the effect of varying composition in a particular alloy under certain conditions may be determined. Figure 12 shows trends with increasing tungsten content, with a maximum at ~3 wt-% for the 10%Cr alloy examined above. Although

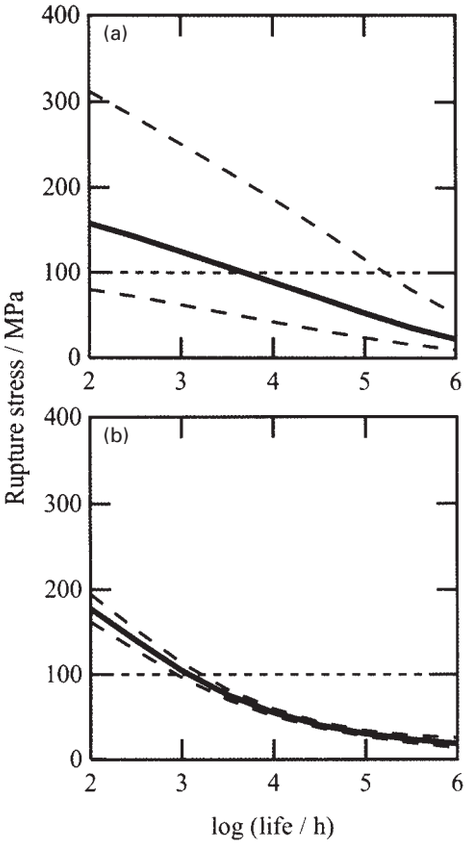

a 3Cr–1·5Mo; *b* 2·25Cr–Mo

10 Comparison of creep rupture stress for 3%Cr and 2·25%Cr steels at 600°C

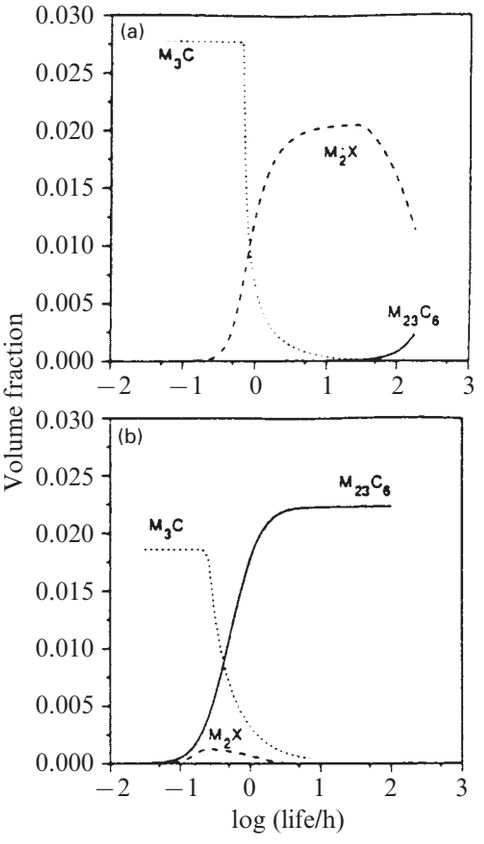

a 2·25%Cr; *b* 3%Cr

11 Plots of calculated carbide volume fraction versus time at 600°C for 2·25%Cr and 3%Cr steels

the uncertainty of the predictions is large, the decline at greater than 3 wt-% is expected as a result of the formation of δ ferrite, which is generally considered detrimental to creep properties. The National Physical Laboratory's metallurgical thermochemistry and thermodynamics database[49] (MTDATA) was used to determine at what weight per cent of tungsten δ ferrite would start to form. The result was 2·7 wt-% tungsten, agreeing well with the neural network results.

APPLICATION TO WELD METALS

It has already been argued above that weld metals and steels of matching composition have similar creep rupture properties. The hypothesis can be proved by examining the relatively limited data on all weld metal tests in the published literature.[5,18] Figure 13 shows the encouraging agreement between calculated values of creep rupture stress and measured values[5] for 2·25Cr–Mo welds (Table 2). The predictions were made without any adjustment to the model, which did not interrogate any weld data during its creation. The heat treatments were changed to represent the welding process and the post-weld heat treatment (PWHT). It was determined, by trial and error, that setting the normalising process to 1200 K for 6 h was a fair representation of the welding process itself. The tempering heat treatment was then set to the conditions of the PWHT and the annealing temperature was set to 300 K to show that no further heat treatments had been carried out.

Figure 13 confirms that it is reasonable to assume that the creep rupture life of weld metals can be modelled on the basis of wrought steels. The results are plotted against varying carbon content because the literature from which these data were taken was, in part, examining the effect of varying carbon weight per cent on weld metals.

The model may also be used to determine creep rupture stress of modern, modified 9Cr–Mo–W weld metals. There is much less information in the open literature about this type of weld metal in terms of creep data, and so there is less opportunity to test the model. Naoi *et al.*[18] have carried out creep tests on a 9Cr–Mo–W gas tungsten arc weld metal, with composition (wt-%) Fe–0·07C–0·20Si–1·01Mn–0·006P–0·004S–8·94Cr–0·48Mo–0·36Ni–0·032N–0·04Nb–0·09V–1·62W. Figure 14 shows that the model is also capable of predicting the creep rupture life of

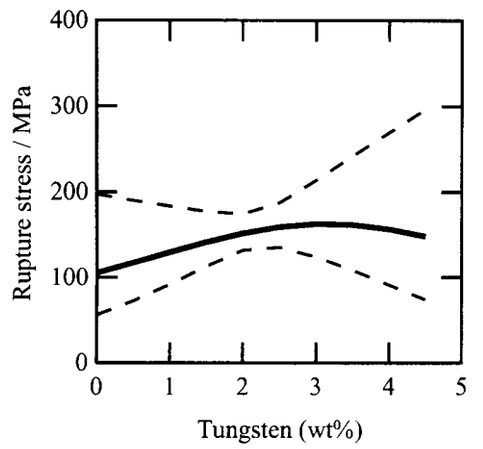

12 Rupture stress for 10Cr–Mo steel with varying tungsten: 550°C for 100 000 h

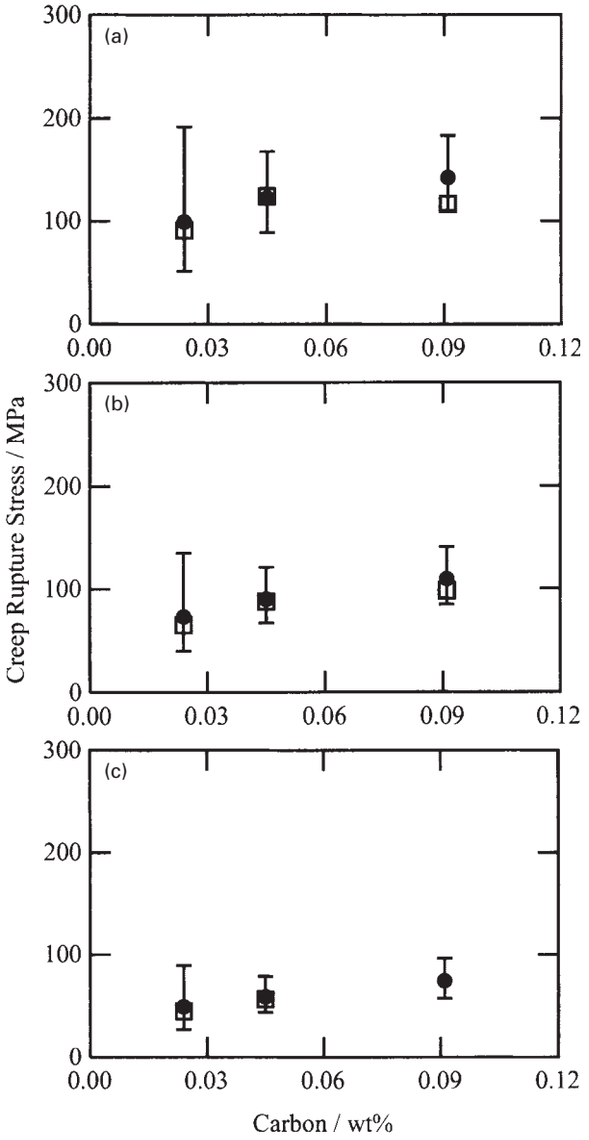

a 510°C; *b* 537°C; *c* 565°C

13 Calculated (filled circles) and measured (open squares) stress rupture data for 2·25Cr–Mo weld metal versus wt-%C: 100 000 h

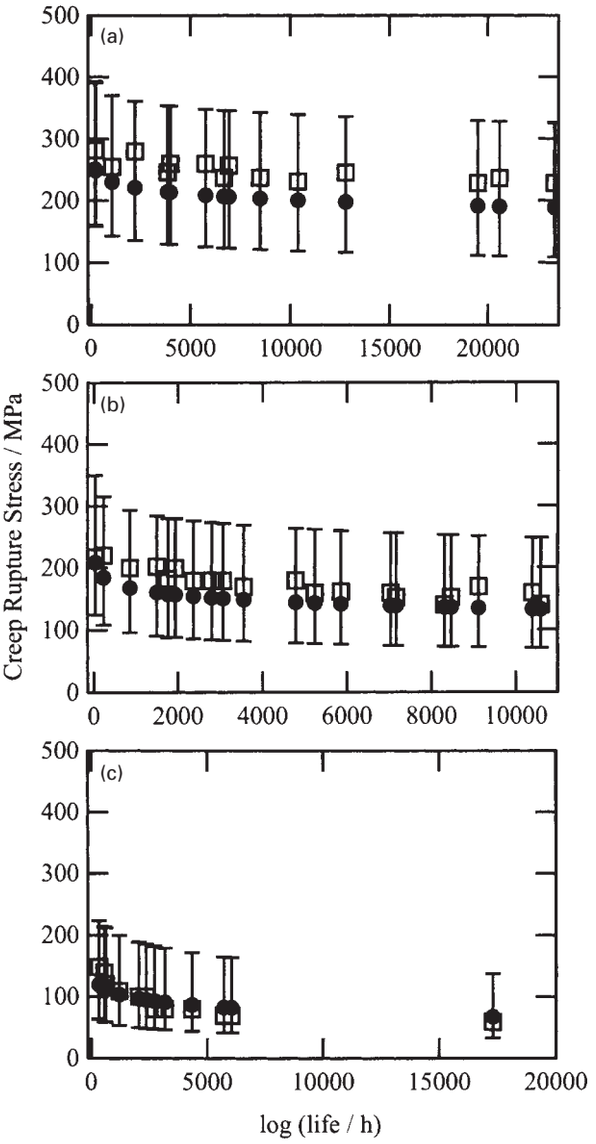

a 550°C; *b* 600°C; *c* 650°C

14 Calculated (filled circles) and measured (open squares) stress rupture data for 9Cr–Mo–W gas tungsten arc weld metal versus creep rupture life

modified 9Cr–Mo–W weld metals. The ability to predict the creep properties of these welds has direct industrial implications, as discussed above.

CONCLUSIONS

A neural network model has been created to study the influence of chemical composition and heat treatment on the creep rupture strength of ferritic steels. The model is based on a very large data set accumulated from the literature.

The model has been successfully applied to weld metal data reported in the literature, even though these were not used in the creation of the model. The present work is helping in the choice of weld metal for the manufacture of small power plant based on a steam turbine.

ACKNOWLEDGEMENTS

The authors are grateful to Rolls-Royce Allen Steam Turbines for financial assistance, and to Professor A. Windle of the University of Cambridge for the provision of laboratory facilities. They would like to acknowledge the generous provision of experimental data by Dr Eng. F. Abe of the National Research Institute for Metals in Japan.

REFERENCES

1. A. G. SHEARD and M. J. RAINE: Proc. Conf. 'International joint power generation', 701–712; 1998, New York, ASME.
2. R. LISTMANN: IMechE Seminar S502, 'Efficient, flexible and economic power generation – the advanced combined cycle technology', Proc. CCGT IV: 'The next generation', April 1997, IMechE.
3. R. N. MASON and A. G. SHEARD: Proc. 5th 'Engineering for profit from waste' Conf., 39–53; 1997, IMechE.
4. H. K. D. H. BHADESHIA: Proc. 5th Int. Conf. on Trends in Welding Research, (ed. J. M. Vitek *et al.*), 795–804; 1999, Materials Park, OH, ASM International.
5. C. D. LUNDIN, S. C. KELLEY, R. MENON, and B. J. KRUSE: *Weld. Res. Counc. Bull.*, 1986, **277**, 1–66.
6. National Research Institute for Metals: NRIM Creep Data Sheets, 1991, 36A; 1986, 3B; 1994, 13B; 1979, 10A; 1981, 19A; 1998, 46; 1998, 10B; 1996, 43; 1997, 19B; 1997, 44; 1992, 12B;

1994, 21B; 1994, 31B; 1990, 35A; 1997, 11B; 1994, 20B; 1976, 2A; 1996, 1B; 1990, 9B.
7. F. MASUYAMA and M. OHGAMI: Proc. Conf. JIMIS-7, Nagoya, Japan, 1993, 325–332.
8. F. ABE and S. NAKAZAWA: *Metall. Trans. A*, 1992, **23A**, 3025–3034.
9. V. SKLENIČKA, K. KUCHAŘOVA, A. DLOUGHÝ, and J. KREJČÍ: in 'Materials for advanced power engineering', (ed. D. Coutsouradis), Part I, 435–444; 1994, Dordrecht, Kluwer Academic Publishers.
10. F. MASUYAMA and T. YOKOYAMA: 'Materials for advanced power engineering', (ed. D. Coutsouradis), Part I, 301–308; 1994, Dordrecht, Kluwer Academic Publishers.
11. L. KUNZ, P. LUKAŠ, and V. SKLENIČKA: in 'Materials for advanced power engineering', (ed. D. Coutsouradis), Part I, 445–452; 1994, Dordrecht, Kluwer Academic Publishers.
12. T. FUJITA: in 'New steels for advanced plant up to 620°C', (ed. E. Metcalfe), 190–200; 1995, Palo Alto, CA, EPRI.
13. B. S. GREENWELL and J. W. TAYLOR: Proc. IMechE Conf. C386/041, 1990, 283–296.
14. J. HALD: in 'New steels for advanced plant up to 620°C', (ed. E. Metcalfe), 152–173; 1995, Palo Alto, CA, EPRI.
15. G. A. HONEYMAN: in 'New steels for advanced plant up to 620°C', (ed. E. Metcalfe), 70–83; 1995, Palo Alto, CA, EPRI.
16. F. BRÜHL, K. HAARMANN, G. KALWA, H. WEBER, and M. ZSCHAU: *VGB Kraftwerkstechnik*, 1989, **69**, 1064–1080.
17. P. J. GROBNER and W. C. HAGEL: *Metall. Trans. A*, 1980, **11A**, 633–642.
18. H. NAOI, H. MIMURA, M. OHGAMI, H. MORIMOTO, T. TANAKA, Y. YAZAKI, and T. FUJITA: in 'New steels for advanced plant up to 620°C', (ed. E. Metcalfe), 8–29; 1995, Palo Alto, CA, EPRI.
19. M. MORINAGA, R. HASHIZUME, and Y. MURATA: in 'Materials for advanced power engineering', (ed. D. Coutsouradis), Part I, 319–328; 1994, Dordrecht, Kluwer Academic Publishers.
20. V. K. SIKKA, M. G. COWGILL, and B. W. ROBERTS: Proc. Topical Conf. on 'Ferritic alloys for use in nuclear technologies', 413–423; 1984, Warrendale, PA, TMS-AIME.
21. M. L. SHAW, T. B. COX, and W. C. LESLIE: *J. Mater. Energy Syst.*, 1987, **8**, 347–355.
22. Y. TSUCHIDA, R. YAMABA, K. TOKUNO, K. HASHIMOTO, T. OGAWA, and T. TAKEDA: Internal report, Nippon Steel Corporation, Japan, 1990.
23. C. COUSSEMENT, M. DE WITTE, A. DHOOGE, R. DOBBELAERE, and E. VAN DER DONCKT: *Rev. Soudure-Lastijdschr.*, 1990, **1**, 58–63.
24. H. MASUMOTO, H. NAOI, T. TAKAHASHI, S. ARAKI, T. OGAWA, and T. FUJITA: Proc. EPRI 2nd Conf., Palo Alto, CA, 1988, 40.3–40.10.
25. V. K. SIKKA and R. H. BALDWIN: 'Data package for modified 9Cr1Mo alloy, update', internal report, Oak Ridge National Laboratories, TN, 1987.
26. A. ISEDA, M. KUBOTA, Y. HAYASE, S. YAMAMOTO, and K. YOSHIKAWA: *Sumitomo Search*, 1988, **36**, 17–29.
27. J. ORR and D. BURTON: in 'Materials for advanced power engineering', (ed. D. Coutsouradis), Part I, 263–280; 1994, Dordrecht, Kluwer Academic Publishers.
28. Internal report, Nippon Kokan KK, Tokyo, 1987.
29. T. FUJITA, K. ASAKURA, T. SAWADA, T. TAKAMATSU, and Y. OTOGURO: *Metall. Trans. A*, 1981, **12A**, 1071–1079.
30. T. FUJITA and N. TAKAHASHI: *Trans. ISIJ*, 1979, **18**, 269–278.
31. A. HIZUME, Y. TAKEDA, H. YOKOTA, Y. TAKANO, A. SUZUKI, S. KINOSHITA, M. KOHNO, and T. TSUCHIYAMA: in 'Advanced materials technology '87', (ed. R. Carson *et al.*), 143–151; 1987, Covina, CA, SAMPE Publishers.
32. K. KUWABARA, A. NITTA, T. OGATA, and S. SUGAI: in 'Advanced materials technology '87', (ed. R. Carson *et al.*), 153–162; 1987, Covina, CA, SAMPE Publishers.
33. K. HAARMANN and G. P. KALWA: in 'Advanced materials technology '87', (ed. R. Carson *et al.*), 267–273; 1987, Covina, CA, SAMPE Publishers.
34. R. VANSTONE: Private communication, 1999.
35. 'Development of high strength 2·25Cr steel tube (HCM25) for boiler applications', Sumitomo Metal Industries, Tokyo, 1993.
36. Y. MURATA, M. MORINAGA, and R. HASHIZUME: in 'Advances in turbine materials, design and manufacturing', Proc. 4th Int. Charles Parsons Turbine Conf., (ed. A. Strang *et al.*), 270–282; 1997, London, The Institute of Materials.
37. 'Procedures to determine maximum allowable stress values for NF616 ferritic steel', Nippon Steel Corp., Tokyo, 1993.
38. 'Procedures to determine allowable stress values for HCM12A ferritic steel tubes and pipe', Sumitomo Metal Industries and Mitsubishi Heavy Industries, Tokyo, 1992.
39. M. OHGAMI, H. MIMURA, H. NAOI, and T. FUJITA: Proc. 5th Int. Conf. on Creep of Materials, Lake Buena Vista, FL, USA, May 1992, 69–73.
40. F. ABE and S. NAKAZAWA: *Mater. Sci. Technol.*, 1992, **8**, (12), 1063–1069.
41. L. W. BUCHANAN, A. N. R. HUNTER, and A. V. HOLT: 'Materials for ultra-supercritical boilers', internal report.
42. H. NAOI, M. OHGAMI, S. ARAKI, T. OGAWA, T. FUJITA, H. MIMURA, M. SAKAKIBARA, Y. SOGOH, and H. SAKURAI: *Nippon Steel Tech. Rep.*, 1993, **57**, 22–27.
43. D. COLE: unpublished work, 1998–99.
44. N. KOMAI, F. MASUYAMA, I. ISHIHARA, T. YOKOYAMA, Y. YAMADERA, H. OKADA, K. MIYATA, and Y. SAWARAGI: in 'Advanced heat resistant steel for power gereration', (ed. R. Viswanathan and J. Nutting), 96–108; 1999, London, IoM Communications.
45. T. FUJITA: *J. Iron Steel Inst. Jpn*, **76**, (7), 1053–1059.
46. F. BRUN, T. YOSHIDA, J. D. ROBSON, V. NARAYAN, H. K. D. H. BHADESHIA, and D. J. C. MACKAY: *Mater. Sci. Technol.*, 1999, **15**, (5), 547–554.
47. D. J. C. MACKAY: in 'Mathematical modelling of weld phenomena 3', (ed. H. Cerjak), 359–389; 1997, London, The Institute of Materials.
48. J. D. ROBSON and H. K. D. H. BHADESHIA: *Calphad*, 1996, **20**, 447–460.
49. 'MTDATA: metallurgical thermochemistry and thermodynamics database', National Physical Laboratory, Teddington, 1996.